Electrochemical reduction of some 2,6-disubstituted pyridine-based esters and thioic *S*-esters in acetonitrile

Richard D. Webster,*[a] Alan M. Bond[a] and Thomas Schmidt[b]
[a] *School of Chemistry, La Trobe University, Bundoora, Victoria 3083, Australia*
[b] *Boehringer Mannheim GmbH, Sandhofer Str. 116, D-68298 Mannheim, Germany*

Voltammetric studies at glassy carbon, gold, mercury, platinum and silver electrodes on 2,6-disubstituted pyridine esters and thioic *S*-esters in acetonitrile have shown that they may be reduced at negative potentials [−1.95 to −2.27 V *vs.* Fc/Fc^+] (Fc = ferrocene). The reduction process corresponds to a chemically reversible one-electron reduction step leading to the formation of a radical anion for many of the compounds at moderately high scan rates (> 1–10 V s^{-1}), but at lower scan rates the process appears chemically irreversible owing to the instability of the radical anion. Reduction is believed to occur in the carbonyl region of the molecules with the thioic *S*-esters being easier to reduce than the esters by *ca.* 300 mV and the reduction potential correlating with the strength of the C=O bond as measured by IR spectroscopy. Controlled potential electrolysis experiments performed on an ester and the analogous thioic *S*-ester showed that reduction of an ester on the long time domain experiments resulted in cleavage of the O–R bond while the thioic *S*-ester cleaved at the C(O)–S bond and underwent further reaction to form interesting and unusual products. The isolated products and mechanism of the reduction, as determined from voltammetric, kinetic, EPR spectroscopy and other spectroscopic data, are discussed in detail. The design and operation of a simple and efficient bulk electrolysis cell used in these experiments is also discussed.

The electrochemical reduction of esters of benzene has been reported by numerous workers and this subject has been reviewed recently in a book by Lund and Baizer.[1] Wagenknecht *et al.*[2] reported that in aprotic media reduction of alkyl benzoate esters results in cleavage of the O–R bond as the major reaction pathway. Falsig and Lund[3] reported on the analogous compound in which the oxygen in the ester is replaced with a sulfur; the carbothioic *S*-esters are reduced to form diphenylacetylene, the benzoate anion and the thiolate. Although the exact mechanism for the reduction is complicated, it would appear that the principal products resulted from cleavage of the C(O)–S bond rather than the S–R bond. In the electrochemically induced rearrangement of *S,S*-diaryl benzene-1,2-dicarbothiates,[4] cleavage of one C(O)–S bond must occur although again the mechanism is complicated. Electrochemically induced cleavage of the C(S)–S bond in thiobenzoate esters has also been reported.[5]

In contrast to the case of esters of benzene, there is little information in the literature regarding the reduction and voltammetry of pyridine-based esters or thioic *S*-esters. Additionally, as far as we are aware there has not been a study that compares and contrasts the electrochemical behaviour of aromatic esters and aromatic thioic *S*-esters. Consequently, in this paper, a number of 2,6-disubstituted esters of pyridine (**1**–**8**) have been selected and their electrochemical behaviour examined and compared in the aprotic solvent acetonitrile using a variety of electrochemical techniques. The compounds are compared with each other on the basis of general cyclic voltammetric behaviour, relative reduction potentials, stability of their associated radical anions formed by reduction and in some cases the products of bulk controlled potential electrolysis experiments. During electrochemical reactions of organic compounds, the intermediates formed are frequently radicals. Therefore, electrolysis experiments were monitored by EPR spectroscopy with the aim of identifying paramagnetic intermediate compounds that provide mechanistic information concerning the reactions.

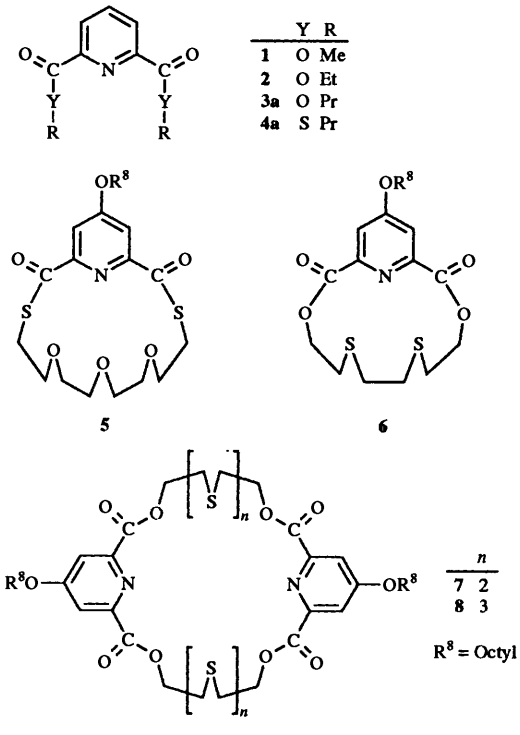

Results and discussion

Voltammetry

Voltammetrically, the compounds behave similarly in that they are all able to be reduced, but not oxidised, within the solvent window available in acetonitrile with Et_4NBF_4 as the supporting electrolyte. Under conditions of cyclic voltammetry (CV), compounds **1**–**6** display a reversible reduction response,

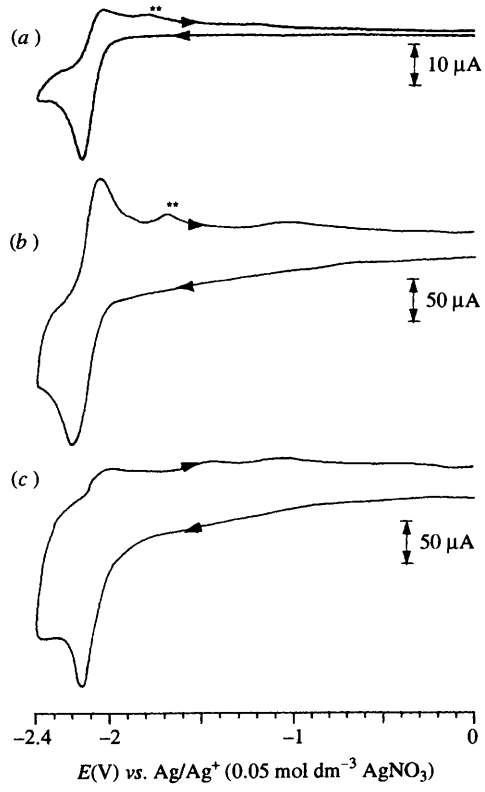

Fig. 1 Cyclic voltammograms at a glassy carbon electrode in MeCN (0.1 mol dm^{-3} Et_4NBF_4) for reduction of (*a*) 1 mmol dm^{-3} compound **3a**, scan rate = 100 mV s^{-1}; (*b*) 1 mmol dm^{-3} compound **3a**, scan rate = 5.120 V s^{-1}; (*c*) 0.5 mmol dm^{-3} compound **8**, scan rate = 51.200 V s^{-1}. * Represents adsorption processes (see text for further details).

provided the scan rate is sufficiently high. At low scan rates the reduction response appears chemically irreversible, *e.g.* in the case of compound **3a**, at a scan rate of 100 mV s^{-1} [Fig. 1(*a*)] considerable irreversibility is observed. However, as the scan rate approaches 5 V s^{-1} the CV becomes chemically reversible [Fig. 1(*b*)]. Hence the irreversibility of voltammograms at low scan rates is due to the reduced species being chemically unstable, not to a low rate of heterogeneous charge transfer between the electrode surface and the molecules. In contrast the voltammetry of compounds **7** and **8** remains completely chemically irreversible up to the maximum scan rate examined of 50 V s^{-1} [Fig. 1(*c*)]. Thus, potentials obtained for these compounds have no direct thermodynamic significance.

Table 1 contains the average calculated (approximately reversible) reduction potentials for the eight compounds obtained from cyclic and differential pulse voltammetric (DPV) experiments at a variety of electrode surfaces in acetonitrile. The reversible reduction potentials for compounds **1–6** were calculated from CV data obtained where the ratio of the oxidative (i_p^{ox}) to reductive (i_p^{red}) peak currents was equal to unity (between 1 and 10 V s^{-1}), and using eqn. (I) where $E^r_{\frac{1}{2}}$ is the

$$E^r_{\frac{1}{2}} = (E_p^{ox} + E_p^{red})/2 \quad \text{(I)}$$

reversible half-wave potential (approximates E^0_f) and E_p^{ox} and E_p^{red} are the oxidation and reduction peak potentials, respectively.

For DPV, a pulse amplitude (ΔE) of −50 mV and a sweep rate of 2 mV s^{-1} was used and the half-wave potential was calculated from eqn. (II). There was no discernible difference

$$E^r_{\frac{1}{2}} = E_p^{red} + [(\Delta E)/2] \quad \text{(II)}$$

in the calculated reduction potential at the different electrode surfaces, within experimental error, so the value recorded in Table 1 was obtained from the average of 10 results at each electrode. The potential range of the CV results was ± 10 mV and for DPV ± 3 mV. The larger range associated with CV is mainly due to the difficulty of measuring accurate peak potentials at moderately high scan rates with macro-scale electrodes where the effects of solution resistance become more significant. Some of the potentials recorded by DPV are slightly more positive than those obtained by CV. This may be due to the presence of a small amount of adsorption which accompanies the electrode process (see later).

Data in Table 1 indicate that the thioic *S*-esters (**4a** and **5**) are reduced at very similar potentials while the esters (**1–3a** and **6–8**) are reduced at potentials which are *ca.* 200–300 mV more negative. Assuming that reduction is occurring directly at the carbonyl group the differences in reduction potential can be explained by differences in the strength of the C=O bond. The esters (**1–3a** and **5–8**) which have the electronegative oxygen next to carbonyl, withdraw electron density from the carbon and hence increase the π backbonding from the oxygen to the carbon in the carbonyl, making the C=O bond stronger and therefore more difficult to reduce. Compounds **4a** and **5** which have the less electronegative sulfur attached to the carbonyl have a relatively weaker C=O bond and are thus easier to reduce. This concept is supported by IR spectroscopy (Table 1). The compounds with oxygen next to the carbonyl have a C=O stretch at a higher frequency (higher energy) than those with a sulfur next to the carbonyl.

It is well established[6] that reduction of organic compounds leads to an electron being added to the lowest unoccupied molecular orbital. For the compounds being considered in this paper it is logical that the additional electron(s) would reside within the π-type aromatic system of the pyridine and carbonyl groups. It is therefore significant that the 4-octyloxy groups do not significantly alter the reduction potential of the compounds, presumably because they are not sufficiently electron withdrawing to affect greatly the electron distribution at the carbonyl group.

Compounds **1–4a**, the simple alkyl esters, displayed further reduction processes at more negative potentials which will be discussed in detail in the section describing data obtained from bulk controlled potential electrolysis experiments.

Number of electrons transferred

Using Ag, GC (glassy carbon) and Pt rotating disc electrodes and current sampled DC polarography at a dropping-mercury electrode, the number of electrons transferred in the first reduction step for compounds **1–6** was calculated from the slope (2.303 *RT*/*nF*) of plots of *E vs.* log[(i_d − *i*)/*i*] (*E* = potential in V, *i* = current and i_d = the limiting current) in the usual manner,[7] by assuming the electron transfer step is reversible. The assumption of reversible electron transfer for compounds **1–6** is reasonable since the $E_{\frac{1}{2}}$ values are independent of the electrode rotation rate and/or drop times. Furthermore, under conditions of CV experiments the E_p^{ox} and E_p^{red} separations of compounds **1–6** at a scan rate of 50 V s^{-1} were similar to those obtained for the Fc/Fc^+ redox couple at the same scan rate. The ferrocene process is a model system of a reversible process. Table 1 lists the results of the electron transfer calculations and indicates that for compounds **1–6** on the short voltammetric timescale ($v \geq 20$ mV s^{-1}) approximately one electron is transferred per molecule. The lower values calculated using the glassy carbon electrode are most likely due to uncompensated resistance resulting from the higher resistance of this electrode material. Lowering the scan rate from 100 mV s^{-1} to 20 mV s^{-1} (rotating disc experiments) made no difference to the result. For compounds **7** and **8** the 'log' plots yielded values for *n*

Table 1 Voltammetric data at 25 °C in acetonitrile (0.1 mol dm^{-3} Et_4NBF_4) for compounds **1–8**

Compound	Calculated $E^{\tau}_{\frac{1}{4}}$ values for first reduction process		Determination of no. of electrons transferred in first reduction process					
	Cyclic voltammetry/ V[a]	Differential pulse voltammetry/ V[a]	Linear sweep voltammetry-rotating disc electrodes[b] Ag	GC	Pt	Current sampled DC polarography[b]	Controlled potential electrolysis[c]	Carbonyl stretching frequency/ cm^{-1}[d]
1	−2.22	−2.22	1.0	0.9	1.0	1.0	1.0	1740br
2	−2.23	−2.22	0.9	0.8	0.9	1.0	0.9	1740br
3	−2.23	−2.22	1.0	0.9	1.0	1.2	0.9	1745s 1721s
4	−1.95	−1.95	1.2	0.9	1.0	1.1	1.2	1667s
5	−1.98	−1.98	1.2	1.0	1.0	1.1	1.1	1670s
6	−2.27	−2.24	1.0	0.8	1.0	1.0	1.0	1719s
7	*e*	−2.18[e]	*e*	*e*	*e*	*e*	1.8	1719s
8	*e*	−2.17[e]	*e*	*e*	*e*	*e*	2.2	1716s

[a] Average reversible reduction potential of the compounds relative to the ferrocene/ferrocenium redox couple calculated from data obtained at Ag, Au, GC, Hg and Pt electrodes (see text). [b] The number of electrons transferred per molecule calculated from the slope of plots of E (V) *versus* log $[(i_d - i)/i]$ and assuming a reversible reduction process. [c] The number of electrons transferred per molecule calculated by coulometry. [d] IR spectra from KBr powder or discs. br = broad, s = sharp. [e] Value could not be calculated or is uncertain in the thermodynamic sense because of the irreversibility of the process (see text).

Table 2 Rate constants for the chemical step(s) following reversible electron transfer for compounds **1–6** (1.0 mmol dm^{-3}), assuming first-order kinetics, calculated at 25 °C in acetonitrile with Et_4BF_4 (0.1 mol dm^{-3}) at a Pt electrode.

Compound	k_f/s^{-1}	Compound	k_f/s^{-1}
1	1.3	**4**	8.4
2	1.3	**5**	0.1
3	1.7	**6**	0.07

considerably less than one (0.6–0.7) indicating irreversible electron transfer behaviour. The number of electrons associated with this step was instead calculated from comparisons of the limiting current. The diffusion-controlled limiting current per unit concentration for compounds **7** and **8** was between 1.3 and 1.5 times the value of the other compounds for the same rotation rate (rotating disc) or drop times (polarography). Thus, assuming similar diffusion coefficients for all compounds and an n-value of 1.0 for compounds **1–6** leads to apparent n values of 1.3–1.5 for compounds **7** and **8**. Considering that compounds **7** and **8** contain twice the number of electroactive functional groups as compounds **1–6** it might be expected that compounds **7** and **8** would undergo a simple two-electron reduction on the short voltammetric timescale. However, the results obtained from the slope of the potential–current curves and from the limiting currents under steady-state conditions indicate that this is not the case and would suggest that compounds **7** and **8** undergo a more complicated reduction mechanism.

For bulk controlled potential electrolysis experiments at a GC electrode, the number of electrons transferred, calculated on the basis of coulometry and use of Faraday's Law, was 1 ± 0.2 for compounds **1–6**. Despite the irreversibility of the process on the long time domain experiments, this result is in agreement with the rotating disc and polarography results, where the process is reversible. The simplest explanation for this observation is that the compounds undergo a simple EC (reversible electron transfer–chemical reaction sequence) mechanism on long time domains and that any intermediate products do not undergo further reduction.

Kinetic measurements

The rate of reaction of compounds **1–6** was calculated for a reversible charge transfer followed by an irreversible chemical step using the method of Nicholson and Shain.[8] The ratio of

$$A + e^- \rightleftharpoons B$$
$$B \xrightarrow{k_f} C$$

i_p^{ox}/i_p^{red} was measured at a variety of scan rates and the k_f value was calculated at each scan rate using a working curve of i_p^{ox}/i_p^{red} *vs.* $k_f\tau$ (ref. 8) (τ is the time in seconds to scan from the switching potential to the $E_{\frac{1}{4}}$). The slope of the plots of $k_f\tau$ *vs.* τ yielded k_f, assuming pseudo-first-order kinetics (Table 2). The results in Table 2 indicate that compound **4a** is the least stable to electrochemical reduction, followed by compounds **1–3a** which show similar reaction rates. Compounds **5** and **6** have the lowest k_f values, possibly because their ring structure acts to stabilise the radical anion, species B, in the scheme above, with the reaction rate for compound **6** being *ca.* 120 times less than that for compound **4a**. The irreversibility of reduction for compounds **7** and **8** made them unsuitable for comparison using this method.

Adsorption effects

Data in Table 1 show that the reduction potentials are largely independent of the electrode material. However, detailed analysis of the responses obtained during CV and linear sweep voltammetry (LSV) indicated that adsorption of the compounds occurs and that this is highly electrode dependent.

Adsorption features associated with voltammetric experiments are evident in two forms. The first type is due to the molecule spontaneously adsorbing to the surface of the electrode before a potential is applied. This form of adsorption gives rise to pre-peaks before the main diffusion-controlled peaks (marked as * in Fig. 2). These responses are recognised as surface-based processes as they display a linear relationship of peak current (i_{ads}) with a scan rate (v) as opposed to the diffusion-controlled processes which display a $v^{\frac{1}{2}}$ relation with i_p [Fig. 2(*a*)–(*d*)]. If the mercury (or solid) electrode is left in solution without renewing the drop (or polishing), the adsorption products build up with time as indicated in Fig. 2(*e*). The adsorption process severely modifies the voltammetry relative to that obtained at a freshly prepared electrode [compare Fig. 2(*c*) and (*e*)]. In addition, in the presence of convection (stirring the solution), adsorption occurs much more rapidly. The compounds containing sulfur (**4a–8**) appear to adsorb more strongly. Of the solid electrodes tests, platinum and glassy carbon surfaces show the least pronounced adsorption features while the influence of adsorption is most

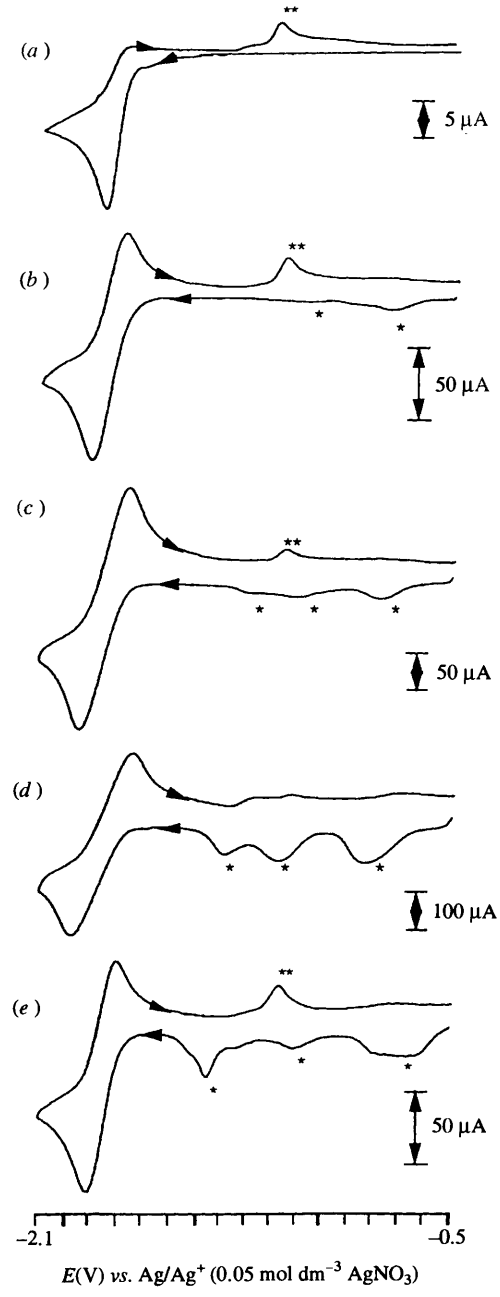

Fig. 2 Cyclic voltammograms of a 1 mmol dm^{-3} solution of compound **4a** at a fresh hanging mercury drop electrode in MeCN (0.1 mol dm^{-3} Et_4NBF_4). Scan rates of (*a*) 0.1, (*b*) 5.120, (*c*) 25.600, (*d*) 51.200 and (*e*) 5.120 V s^{-1} after adsorptive accumulation of reactants. * and ** represent absorption based processes (see text for further details).

complicated on mercury. Mercury has long been known to interact with sulfur containing compounds and the adsorption of sulfur-based compounds would be expected to be the strongest at this electrode. However, it is unknown whether the adsorbed materials retain their identity on the electrode surface or dissociate.

The second form of adsorption is observed on the reverse (oxidation) scan of cyclic voltammograms (marked ** in Figs. 1 and 2). The peak potential for this adsorption process depends on the electrode surface. It is most likely associated with adsorption of the reduced form of the compound as has been reported on numerous occasions for other carbonyl compounds.[1,9] In general the adsorption peak decreases in size with increasing scan rate because the reduced form has less time for specific interaction with the electrode.

Note that the presence of adsorption could lead to errors in the values of k_f listed in Table 2. To minimise this problem kinetic measurements are reported from data obtained at a Pt electrode where adsorption is minimal. Furthermore, the electrode was polished frequently.

Bulk controlled potential electrolysis experiments (CPE)

Preparative scale CPE at a GC electrode was performed on compounds **3a** and **4a** in order to compare the products of the electrolysis of an ester and the corresponding thioic *S*-ester. Electrolysis experiments were conducted at least in triplicate to ensure consistency of results. Compounds **5–8** were insufficiently soluble in acetonitrile to enable preparative scale experiments to be performed.

The one electron bulk reduction of compound **3a** produced the carboxylate anion (**3b**) (structure given in Scheme 1) in high

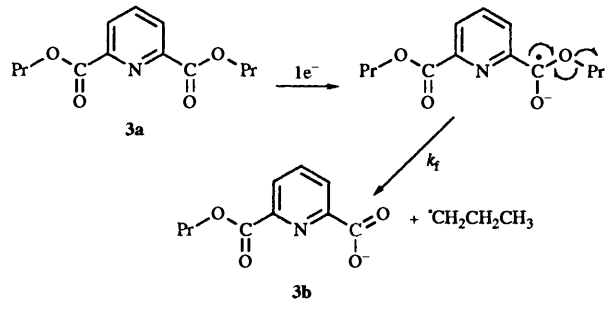

Scheme 1

yield. This compound results from cleavage of one of the O–R bonds [Fig. 3(*a*) and (*b*)]. A plausible mechanism for this reaction, as shown in Scheme 1, involves initial reduction at the carbonyl group followed by elimination of a propyl radical to leave the stable anionic form of the ester. The reason only one ester group undergoes the cleavage reaction is probably a consequence of the extra negative charge situated on the molecule after the first electron step. This is likely to raise the activation energy required to add another electron or increase the free energy of the final product so as to make further reduction more difficult. A CV of the solution at the completion of the reductive electrolysis [Fig. 3(*b*)] showed that **3b** produced by reduction was harder to reduce than the starting material by *ca.* 200 mV. Methylation of the electrolysis solution by reaction with methyl iodide formed methyl propyl pyridine-2,6-dicarboxylate (**3d**) [Fig. 3(*d*)]. **3d** Is reduced at almost the same potential as the starting material which was to be expected as the dipropyl, diethyl and dimethyl pyridine esters all showed nearly identical electrochemistry. Applying a more negative potential (−2.5 V *vs.* Ag/Ag^+) and a further one-electron reduction of **3b** leads to the formation of the dicarboxylate dianion (**3c**) which upon methylation leads to dimethyl pyridine-2,6-dicarboxylate (**1**) [Fig. 3(*e*)]. (The relative ease of methylation of the quaternary ammonium carboxylates is most likely due to the presence of the supporting electrolyte enhancing the alkylation.[10]) Plots of E *vs.* $\log[(i_d - i)/i]$ showed that compound **3b** also undergoes a reversible reduction. Using cyclic voltammetry at scan rates of up to 50 V s^{-1} failed to obtain i_p^{ox}/i_p^{red} ratios greater than 0.5, which make kinetic evaluation by the method of Nicholson and Shain[8] inaccurate. However, this result shows that the stability of the carboxylate radical anion produced in the second reduction step is substantially less stable than the carboxylate radical anion produced in the first one-electron reduction.

The oxidation responses shown in Fig. 3(*a*) (prior to bulk electrolysis) on the reverse scan of the CV are only observed if the scan is applied in the negative potential direction first. These processes are due to the oxidation of any products formed at the

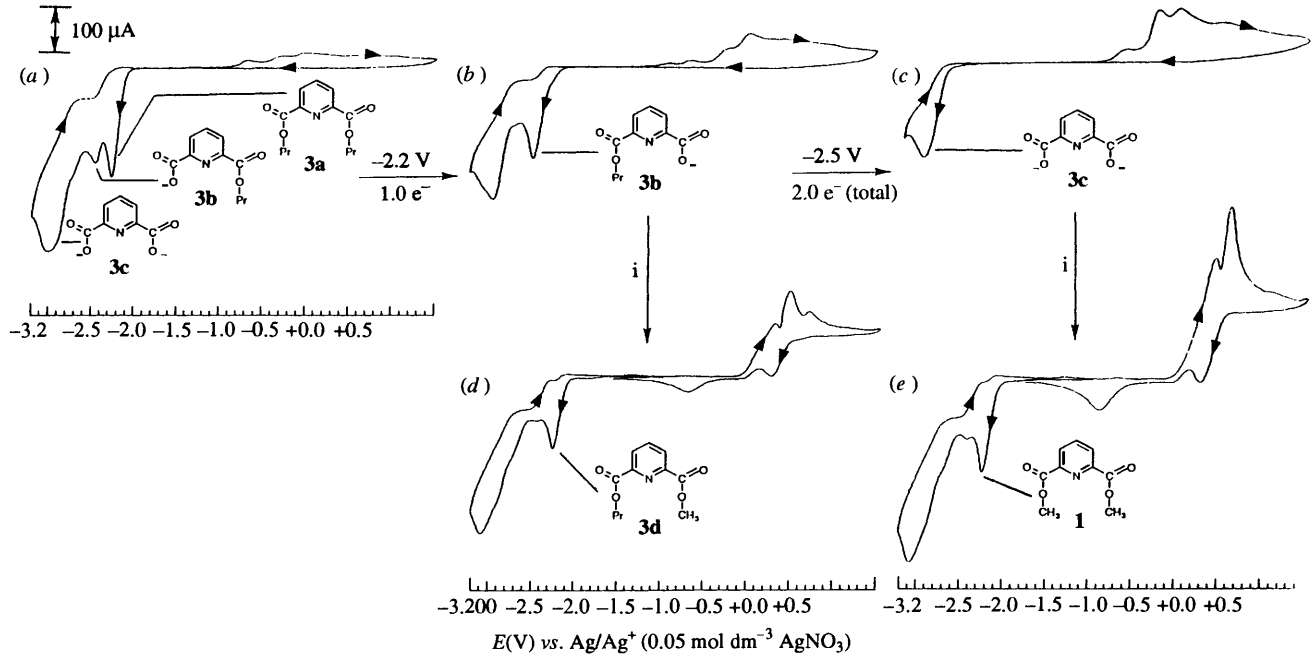

Fig. 3 Cyclic voltammetric responses obtained at a glassy carbon electrode during different stages of bulk reductive electrolysis (at a glassy carbon cup electrode) of a 10 mmol dm^{-3} solution of compound **3a** in MeCN (0.1 mol dm^{-3} Et_4NBF_4). In each case the initial potential was −1.0 V (*vs.* Ag/Ag^+) and the scan rate 100 mV s^{-1}, with the scan initially applied in the negative direction. (*a*) Before electrolysis. (*b*) After the transfer of 1.0 electron per molecule. (*c*) After the transfer of 2 electrons per molecule. (*d*) After methylation at the one electron reduction stage. (*e*) After methylation at the two electron reduction stage. In each case the counter ion for the charged compound formed is the supporting electrolyte tetraethylammonium cation. The species undergoing oxidation at 0.5 V (*vs.* Ag/Ag^+) in (*d*) and (*e*) is free iodide remaining after methylation with methyl iodide. *Reagents and conditions*: (i) MeI, room temp., 24 h.

electrode surface *via* the reduction of the compound. After bulk electrolysis has commenced [Fig. 3(*b*) and (*c*)] the product(s) are present in the bulk solution and their electrochemistry now can be observed voltammetrically by linear sweep voltammetry and scanning only in the positive potential direction. After methylation with methyl iodide the peaks for the reduction products decrease in size. The species undergoing oxidation at *ca.* 0.5 V in Fig. 3(*d*) and (*e*) is the free iodide remaining after methylation with methyl iodide.

Examination of the electrolyte–product mixture by ^1H NMR spectroscopy in the alkyl region after both the one and two electron bulk reductions were completed failed to reveal the presence of species other than the carboxylates. This implies that the cleaved propyl radical groups had combined to give a volatile hydrocarbon, such as hexane. During the bulk electrolysis experiment, only while a potential was applied to the solution, a volatile liquid was observed to collect briefly on the glass lid of the electrolysis cell.

Gul'tyai *et al.*[11] reported that the reduction of methyl benzoate in DMF leads to the carboxylate anion *via* cleavage of the O–R bond in 100% yield which is the same mechanism as we found for the pyridine disubstituted esters. In contrast, Wagenknecht *et al.*[2] found in the electrochemical reduction of *tert*-butyl benzoate that, as well as the formation of the benzoate anion, *tert*-butyl *p*-*tert*-butylbenzoate was also isolated. Therefore it appears that the properties of the cleaved alkyl group determine to a certain extent the products of the bulk electrochemical reduction of aromatic esters. The propyl radicals formed during the reduction of **3a** do not appear to react further with the starting material or the carboxylate anions formed (**3b** or **3c**).

The reduction of compound **4a** was more complicated than for the corresponding ester and two principal products were isolated after methylation in high yields; methyl 6-(propylsulfanyl)carbonylpyridine-2-carboxylate (**4f**) and *S*-propyl 5-methyl-7-oxo-5-[5-(propylsulfanylcarbonyl)pyridin-2-yl]-5,7-dihydrofuro[3,4-*b*]pyridine-2-carbothioate (**4j**). As soon as the potential was applied at the beginning of the bulk electrolysis, the colourless solution changed to a very dark red colour and then rapidly progressed to a black colour. At the end of the electrolysis, even after methylation and stirring, it took several hours for the solution to fade to an orange–red colour. Both of the methylated products isolated from the reaction mixture were white. Schemes 2 and 3 show a postulated mechanism based on all the available experimental evidence for the formation of the two products. Numbers in italics represent possible intermediate compounds. For simplicity in describing the reaction mechanisms, negative charges and unpaired electrons are drawn as isolated on the individual atoms where in reality delocalisation would often occur.

For both products the first step in the reaction, after heterogenous electron transfer, would appear to be cleavage of the C(O)–S bond [Scheme 2, reaction (1)] to form compound **4c**, in contrast to the ester where cleavage of the O–R bond occurred. There is voltammetric evidence in the form of a reduction peak, which increases in size during the electrolysis, of an intermediate compound **4d** from which **4e** is formed [reaction (2)]. The new voltammetric peak corresponding to **4d** occurs at 60 mV more negative potential than **4a**. Therefore the reductive potential applied was controlled carefully so as not to reduce this newly formed species by applying a potential within 5 mV of the $E_{\frac{1}{2}}$ of compound **4a**. If at the completion of the electrolysis the solution is exposed to the atmosphere then the voltammetric reduction peak for **4d** decreases in size and the new peak, which has been identified as corresponding to the reduction of compound **4e**, increases. In addition, if a small amount of water is added to the electrolysis solution at the commencement of the bulk reduction, compound **4e** can be observed voltammetrically to form immediately. Thus compound **4e** results from the reaction of reduced **4a** with water or from the aerial oxidation of an intermediate compound **4d** [reaction (3) and (4)]. Compound **4d** has been tentatively

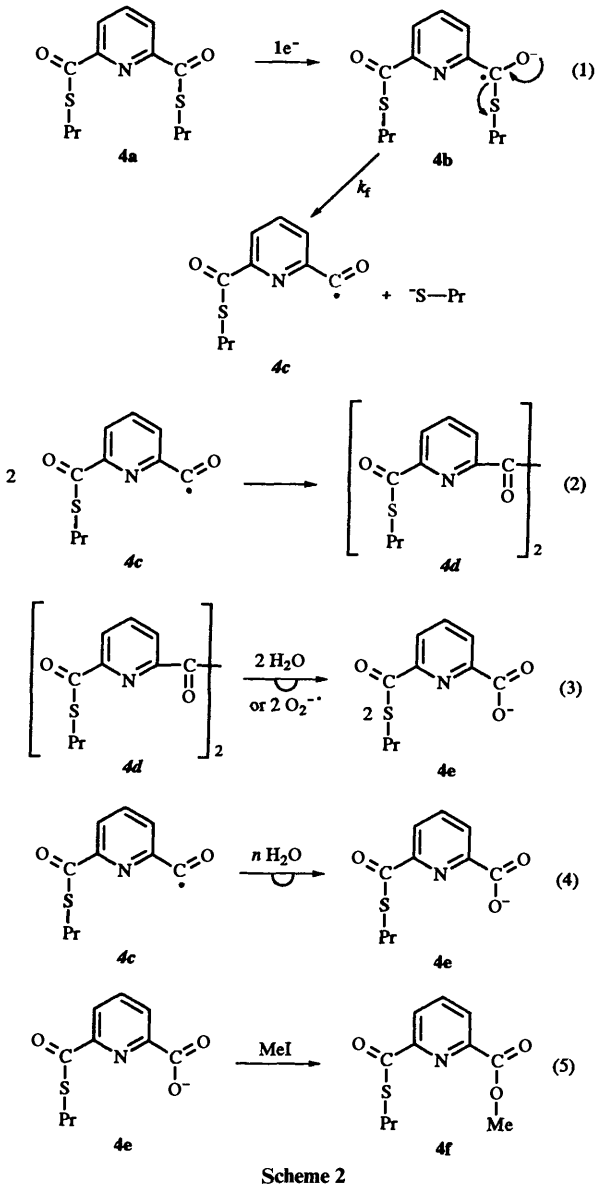

Scheme 2

assigned as an α-diketone, which are susceptible to oxidation at least in aqueous media,[12] and are known to react to form carboxylates in the presence of superoxide.[13] Methylation of **4e** leads to **4f** [reaction (5)]. It made no difference to the products obtained at the end of the electrolysis whether the solution was methylated then exposed to the atmosphere or *vice versa*. However, extraction of the products was easier if oxidation was allowed to occur first. Compound **4e** can also be formed from the reaction of **4a** with trace amounts of superoxide which has been reported for both aromatic and alkyl esters.[14] (The compounds are all more difficult to reduce than oxygen, therefore any dissolved oxygen in solution at the electrode surface during the electrolysis will be converted to superoxide. This reaction for the formation of **4e** should be slight, however, as the solutions were thoroughly degassed with nitrogen before and during the electrolysis.)

The mechanism for the formation of compound **4j** can be formulated to involve, instead of coupling of two carbonyl radical anions, either the nucleophilic attack of one carbonyl radical at the aromatic ring of a starting molecule, or the nucleophilic attack of a carbonyl radical at the aromatic ring of another radical (Scheme 3). In the former case **4c** combines with **4a** to form the radical anion **4g** [reaction (6)]. A further one-electron reduction of **4g** and rearrangement [reactions (7) and (8)] could lead to the anionic lactone. This mechanism requires that **4g** can be reduced at a potential no more negative than **4a** can be reduced at. The propanesulfanyl groups on compound **4g** are non-equivalent and thus reduction will occur only at the one that is easiest to reduce. Overall the reaction would be an ECED mechanism. However, providing the CE step is slow the k_f value obtained by Nicholson and Shain's method[8] is still a good approximation of the rate constant for the formation of compound **4c** if this mechanism is operative. In the latter case two of **4c** could combine directly by nucleophilic attack of one radical on the aromatic ring of another radical to form **4h**, which is still overall an EC mechanism. The EPR spectroscopy of an intermediate paramagnetic compound obtained during the electrolysis of **4a** is discussed below and contains some evidence as to which of the two mechanisms for the formation of **4i** is operative. Subsequent methylation

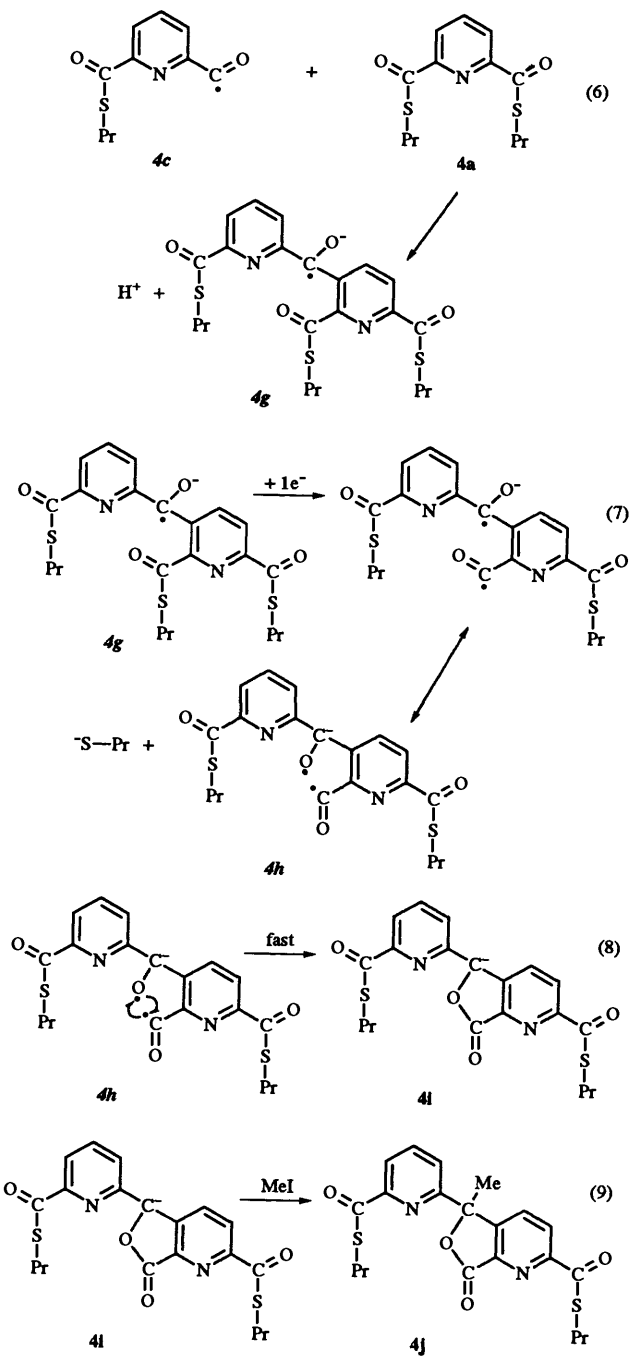

Scheme 3

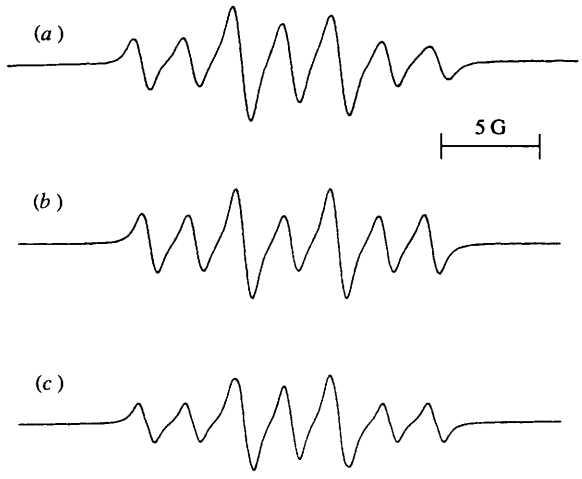

Fig. 4 (*a*) *In situ* first-derivative EPR spectrum obtained during reductive electrolysis at a platinum electrode of a 5 mmol dm^{-3} solution of compound **4a** at room temperature in MeCN (0.1 mol dm^{-3} Et_4NBF_4). The modulation amplitude = 0.2 G and modulation frequency = 50 kHz [g = 2.0048 (±0.0002)]. (*b*) Simulated EPR spectrum with hyperfine splitting constants for two non-equivalent nitrogen atoms of 5.3 G and 2.53 G and for five protons of 0.20 G. (*c*) Simulated EPR spectrum with hyperfine splitting constants for one nitrogen of 2.53 G and three protons of 5.55 G, 5.40 G and 0.40 G. Simulations were calculated with a 100% Lorentzian line shape with a peak-to-peak linewidth of 1.0 G. 1 G = 10^{-4} T.

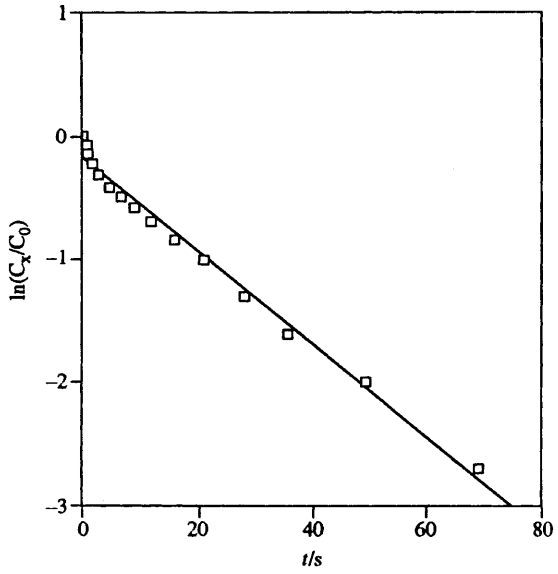

Fig. 5 Plot of $\ln(C_x/C_0)$ (C_0 = signal intensity at time t = 0 and C_x = signal intensity at time t) *vs.* t (s) measured by a time sweep EPR experiment during the decay of a radical obtained by the reductive electrolysis of compound **4a** in MeCN at 20 (±1) °C. Y intercept = −0.17, slope = −0.04, correlation coefficient (R^2) = 0.989.

[reaction (9)] would result in compound **4j**. Dithiolphthalates are known to undergo isomerisation to lactones on heating[15] and also *via* electrochemically induced rearrangement as reported by Praefcke *et al.*,[4] although the dimer-type coupling proposed in this work has not been reported.

TLC experiments indicated that there were at least four other very polar compounds present in the reduced solutions. However, the results of ^{1}H NMR spectroscopy indicated that compounds **4f** and **4j** accounted for a high percentage of the signal intensity in the aromatic region (90–95%) and therefore the extra products were most likely side products formed from the cleaved thiol chains.

EPR spectroscopy

In order to identify possible paramagnetic radical intermediate products formed during the reduction process, *in situ* EPR–electrochemical experiments with a Pt working electrode were undertaken on compounds **3a** and **4a**. Spectra were recorded at room temperature (*ca.* 20 °C) in acetonitrile and also at 203 K in dichloromethane. No EPR spectra were obtained from the reduction of compound **3a** presumably because the radical produced was too short-lived, but a high resolution spectrum of a radical was obtained during the electrolysis of compound **4a** in acetonitrile which is shown in Fig. 4(*a*). An almost identical spectrum was obtained in dichloromethane at 203 K.

The rate constant for the decay of the radical in acetonitrile at *ca.* 20 °C was calculated by electrochemically generating the radical, halting the electrolysis and measuring at constant field the signal intensity by time sweep EPR experiments. The slope of a plot of $\ln(C_x/C_0)$ *vs.* t (C_0 = signal intensity at t = 0 and C_x = signal intensity at varying t) yielded a k_f value of 0.04 s^{-1} and a $t_{\frac{1}{2}}$ of 17 s, assuming first-order kinetics. The decay was controlled so as to occur over a period of 2.5 min thus reducing the effect of diffusion of the radical out of the most sensitive part of the cavity which would alter the signal intensity and affect the signal intensity *vs.* time curve. The first-order plot is provided in Fig. 5. Plots which included terms for second-order kinetics exhibited a much poorer fit to the data. The graph in Fig. 5 displays a small degree of curvature at low values of t which introduces an error to the value of k_f obtained by this method. However, the value of k_f obtained is *ca.* 200 times less than what was obtained voltammetrically by scan rate studies for the rate constant of compound **4b** reacting to form other compounds. This discrepancy is considerably greater than the error for k_f of the radical decomposing, even if more complicated kinetics are involved, and suggests that the radical detected cannot be compound **4b**, but rather another intermediate species.†

Examination of Schemes 2 and 3 indicates that their are two other possibilities for the radical detected; the neutral radical **4c** or the radical anion **4g**. For heterocyclic compounds the coupling constants of nitrogen atoms typically range from 2–8 G and for ring protons can vary from < 1–10 G.[16] For **4g** a simulated spectrum [Fig. 4(*b*)] was calculated on the basis that the nitrogen coupling was > 2 G. The seven line spectra could be simulated almost entirely by considering coupling to the two non-equivalent nitrogen atoms only. However, even with the broad linewidth observed experimentally, this model required that the individual ring-proton coupling does not exceed 0.25 G (alkyl protons were disregarded) which is very unlikely considering that there are five non-equivalent ring protons. For compound **4c** a simulated spectrum could be calculated [Fig. 4(*c*)] which matches that observed experimentally if two of the ring protons have very similar hyperfine splitting constants (*ca.* 5.4–5.6 G) and the nitrogen atom a hyperfine splitting constant of 2.5–2.6 G. If the remaining ring proton and alkyl coupling does not exceed 0.5 G the spectra would not be altered greatly. Hyperfine splitting constants of this magnitude are resonable for pyridine esters.[17] Therefore it appears that the radical detected is more likely to be **4c** than **4g** (or any other dimer type radical) and, as this species has been shown to have some

† We have studied the voltammetry and EPR spectroscopy of a large number of pyridine and benzene ester radicals (unpublished data), and have shown, by cyclic voltammetry, that they are considerably more stable than the compounds under study in this paper. The EPR spectra obtained from some of these radicals are notably less intense than the radical anion described in this report, which supports the data obtained by kinetic means that the radical anion detected *via* the reduction of compound **4a** cannot be the primary radical anion **4b**.

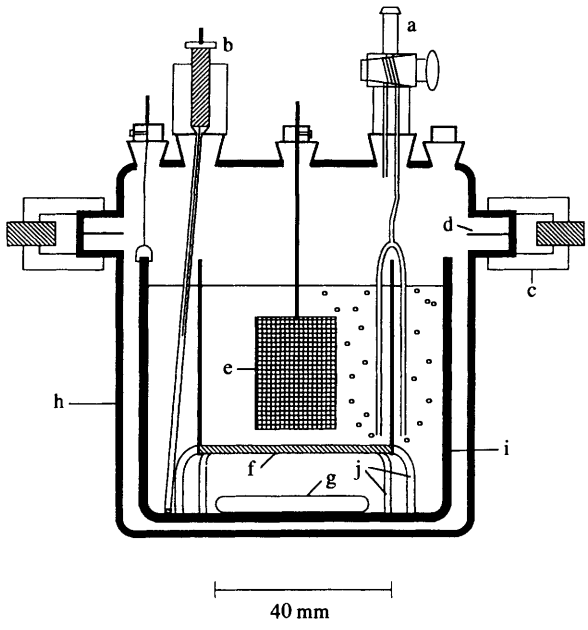

Fig. 6 Schematic diagram of controlled potential electrolysis cell and associated experimental arrangement used for electrochemical synthesis experiments: (*a*) nitrogen gas bubbler, (*b*) Ag/Ag^+ reference electrode, (*c*) spring clamp, (*d*) teflon o-ring, (*e*) platinum basket auxiliary electrode within inner solution compartment, (*f*) 1.0–1.7 μm porosity glass frit, (*g*) magnetic stirrer bar, (*h*) glass outer housing, (*i*) glassy carbon cup working electrode forming outer solution compartment and (*j*) glass supports for counter electrode compartment.

stability (EPR time sweep experiments) and there is no evidence of a radical dimer, the mechanism for the formation of **4i** involving a radical–radical reaction (not a coupling reaction, rather a nucleophilic aromatic substitution) (EC) is more favourable than the alternative ECED mechanism.

The simulated spectra were calculated with 100% Lorentzian lineshape, which is the expected line shape for a free radical with unhindered rotation at room temperature,[18] and with a peak-to-peak linewidth of 1.00 G. The *g*-value was calculated from the difference in magnetic field from a pure crystal of 2,2-diphenyl-1-picrylhydrazyl (2.0037 ± 0.0002 at room temperature)[19] and was 2.0048 ± 0.0002 in MeCN.

Conclusions

The 2,6-disubstituted pyridine alkyl esters and thioic *S*-esters (compounds **1–6**) undergo a one-electron reduction process on both the short (CV 0.02–50 V s^{-1}) and the long (CPE) electrochemical timescales in acetonitrile. In contrast the larger dimer type esters (**7** and **8**) do not undergo simple reversible electrochemical behaviour. Controlled potential electrolysis experiments performed on an ester resulted in the stepwise cleavage of the propyl radicals to form the monoanionic carboxylate and then dianionic dicarboxylate by an EC mechanism. This is an analogous reaction to that reported for some benzoate esters where the formation of the carboxylate anion occurs in high yield. The corresponding thioic *S*-ester reacted with cleavage of the C(O)–S bond followed by further reaction. Although the products of the electrochemical reduction are different to those that have been reported previously for aromatic thioic *S*-esters, the cleavage of the C(O)–S bond as the primary reaction pathway is consistent with other studies. An EPR spectrum obtained during the electrolysis of the thioic *S*-ester showed the formation of a semi-stable ($t_{\frac{1}{2}}$ *ca.* 17 s) radical monomer intermediate which is supportive of an EC rather than an ECED mechanism for the formation of one of the products.

Experimental

Chemicals, solvents and other reagents

Dimethyl (**1**), diethyl (**2**) and dipropyl (**3**) pyridine-2,6-dicarboxylates were prepared by refluxing pyridine-2,6-dicarboxylic acid in thionyl chloride to make the acid chloride and then in the corresponding alcohol to form the diester. The preparation of compound **4a** is to be described elsewhere[20] and **5–8**[21] have been described previously. Purity of the compounds was confirmed by NMR spectroscopy, mass spectrometry, TLC and melting points of the solids. For electrochemical experiments, HPLC grade acetonitrile (MeCN) was purified immediately prior to use by passing through a column of activated neutral alumina.[22] Electrochemical grade tetraethylammonium tetrafluoroborate (Et_4NBF_4), which was used as the supporting electrolyte, was dried *in vacuo* prior to use.

Instrumentation other than voltammetric

IR spectra were recorded with a Model 1720X Perkin-Elmer FT-IR spectrophotometer. Electron ionisation (EI) at 70 eV and chemical ionisation (CI) with methane as the reagent gas, mass spectra were recorded on a Hewlett-Packard 5988A mass spectrometer with an RTE-A data system. ^1H and ^{13}C NMR spectra were recorded on a Bruker AM-300 spectrometer with $CDCl_3$ or $[(CD)_3SO]$ and referenced to the solvent. *J* values are given in Hz. EPR spectra were recorded on a Bruker ECS-106 spectrometer in an *in situ* electrochemical EPR cell which has been described elsewhere.[23] EPR simulations were calculated using the Bruker software (ESP 1600-EPR CALC). TLC analysis was performed on Merck SiO_2 60 F_{254} precoated aluminium sheets visualised with UV light. Elemental analyses were performed at the Chemistry Department, University of Otago, Dunedin, New Zealand.

Voltammetric techniques

Cyclic voltammetry (CV), linear sweep voltammetry (LSV) and differential pulse voltammetry (DPV) measurements were conducted with a BAS 100 or BAS 100A (Bioanalytical Systems) Electrochemical Analyser using a three electrode arrangement. Working electrodes were of macro-dimensions (1–3 mm diameter), consisting of a Metrohm model E 410 hanging mercury drop electrode (HMDE), a glassy carbon disc (GC), a silver disc (Ag), a gold disc (Au) or a platinum disc (Pt). For experiments with a rotating disc electrode, a Metrohm model 628-10 drive unit was used in conjunction with a Metrohm Ag, GC and Pt electrodes. Disc electrodes were frequently polished with a water–diamond paste (1 μm abrasive) slurry and then rinsed with acetonitrile. Polarograms were recorded with a Metrohm 646 VA Processor and a 647 stand with a mercury drop time of 0.8 s.

For CV, LSV, DPV and current sampled DC polarography (DCP) the auxiliary electrode consisted of a Pt wire. To avoid contamination a double junction Ag/Ag^+ (0.05 mol dm^{-3} $AgNO_3$) reference electrode was used. Accurate potentials were recorded relative to the ferrocene/ferrocinium (Fc/Fc^+) redox couple which was used as an internal standard. Test solutions were thermostatted to 25 ± 0.2 °C and were degassed with solvent saturated nitrogen and a continuous stream of nitrogen was passed over the solution while measurements were performed. In all cases the concentration of the supporting electrolyte was 0.1 mol dm^{-3}.

Two types of cell design were employed for CPE experiments. For synthetic scale CPE (gram quantities) a glassy carbon cup (*ca.* 186 cm^2) was used as the working electrode with a platinum mesh basket as the auxiliary electrode. The high powered BAS SP-2 potentiostat had to be used for the larger currents generated in these synthetic experiments. A diagram of the electrolysis cell is given in Fig. 6. The working and auxiliary

electrode compartments were separated by a 1.0–1.7 μm porosity glass frit. The large surface area of the frit was important to enable adequate current to be passed between the working and auxiliary electrodes with typical current levels being 0.2–0.3 A. The position of the glass frit determines that most of the electrolysis occurs at the base of the glassy carbon electrode and not at the sides. Therefore the glassy carbon electrode could be replaced with a mercury pool if required without greatly altering the performance of the cell. The volume of the working electrode compartment is *ca.* 100 cm^3 and the counter electrode compartment *ca.* 65 cm^3. The design of the cell is such that the auxiliary electrode is symmetrically arranged with respect to the working electrode while the Ag/Ag^+ (0.05 mol dm^{-3} $AgNO_3$) reference electrode was positioned so that the glass frit at the tip was as close to the working electrode as possible.[24] The auxiliary and working electrode compartments were degassed with solvent-saturated nitrogen for 1 h before the electrolysis was commenced and the purging continued until the completion of the electrolysis. The working electrode compartment was stirred with a magnetic stirrer bar at as great a rate as possible without causing mixing of the two solutions through splashing.

The level of mixing of the working and auxiliary electrode compartments was tested by adding fluorescein dye to the working electrode compartment and monitoring the change in colour of the counter electrode compartment with time by UV–VIS spectroscopy. After 6 h of continual stirring and purging, a 10% mixing of the solutions occurred using the 1.0–1.7 μm porosity glass frit. Considering that one gram of analyte was able to be electrolysed in 100 cm^3 of solvent with 0.1 mol dm^{-3} supporting electrolyte with a typical exhaustive electrolysis time of 1 h, we estimate that including pre-electrolysis purging time there is 3–4% loss of product due to mixing, assuming that bulk migration is the same as for the dye. Using a 10–20 μm porosity glass frit there was a small increase in the amount of current passed, but a much larger increase in the amount of mixing (nearly 40% after 3 h) making the use of a larger porosity frit unacceptable with this cell design.

For coulometry measurements used to determine *n*-values associated with the electron-transfer process, a cell similar in design, but much smaller than the one described above was used. For this cell a 5 cm^3 inner compartment contained a glassy carbon cylindrical electrode (*ca.* 28 cm^2) as the cathode and a Ag/Ag^+ (0.05 mol dm^{-3} $AgNO_3$) reference electrode, separated by a 1.0–1.7 μm sintered glass frit from a platinum mesh cylindrical electrode used as the anode in the outer compartment. A 3 mm (diameter) GC or Pt electrode was inserted in the working electrode compartment enabling *in situ* cyclic voltammograms to be recorded at different stages of the electrolysis. Solutions were purged with solvent-saturated nitrogen prior to and during electrolysis. Exhaustive electrolysis of a 10 mmol dm^{-3} solution of analyte took *ca.* 3–10 min depending on the number of electrons involved.

General procedure for synthetic scale electrochemical reductions

The potential for the reduction was set by taking an aliquot of solution from the working electrode compartment, diluting to *ca.* 1 mmol dm^{-3} and recording a cyclic voltammogram, using the same reference electrode as that used in the CPE cell. The electrolysis experiment was monitored by taking samples from the working electrode compartment at intervals and recording cyclic voltammograms. At the completion of the reductions, 2 mol equiv. of methyl iodide was added and the solution stirred for 30 min. The reduced solution was then transferred to a volumetric flask and the solution further stirred for 24 h. The acetonitrile was removed and a sample of the resulting electrolyte–product mixture taken for a yield estimate using quantitative ^1H NMR spectroscopy. The combined electrolyte–product mixture was dissolved with 50 cm^3 DMF and further diluted with 30 cm^3 water and the methylated products extracted using diethyl ether. Mixtures of products were further purified using radial chromatography on silica gel with diethyl ether–light petroleum (bp 60–90 °C) (3:17) as the eluent.

Reduction of dipropyl pyridine-2,6-dicarboxylate. 1.5 g of **3a** (6.0 mmol) was reduced at −2.25 V (*vs.* Ag/Ag^+) to form after methylation methyl propylpyridine-2,6-dicarboxylate (**3b**) (1.27 g, 95%). Recrystallised from light petroleum (bp 60–90 °C), mp 58–61 °C; ν_{max}(KBr)/cm^{-1} 1732 and 1743 [O–C(O)]; δ_H(300 MHz; $CDCl_3$) 1.00 (3 H, t, *J* 7.4, CH_2CH_3), 1.83 (2 H, m, *J* 7.2, CH_2CH_3), 3.99 (3 H, s, O–CH_3), 4.36 (2 H, t, *J* 6.9, O–CH_2), 7.99 (1 H, t, *J* 7.8, Ar 4-H) and 8.26 (2 H, m, Ar 3-H and 5-H); δ_C(300 MHz; $CDCl_3$) 10.28 (CH_2CH_3), 21.89 (CH_2CH_3), 53.02 (O–CH_3), 67.75 (O–CH_2), 127.75 and 127.83 (Ar C-3 and C-5), 138.22 (Ar C-4), 148.17 and 148.43 (Ar C-2 and C-6); *m/z* 223 (M^+, 1%), 165 (38), 151 (40), 137 (100), 105 (74), 77 (32) and 41 (15).

Compound **3b** was further reduced at −2.5 V (*vs.* Ag/Ag^+) to form (after methylation) dimethylpyridine-2,6-dicarboxylate (**1**) (1.05 g, 90%). Analytical and spectral data obtained were identical to an authentic sample.

Reduction of *S*,*S*-dipropyl pyridine-2,6-dicarbothioate. 1.5 g (5.3 mmol) of **4a**, TLC [diethyl ether–light petroleum (bp 60–90 °C) (1:1)] R_f 0.68, was reduced at −1.945 to −1.955 V (*vs.* Fc/Fc^+) to form (after methylation) methyl 6-(propylsulfanyl)-carbonylpyridine-2-carboxylate (**4f**) (0.69 g, 55%) and *S*-propyl 5-methyl-7-oxo-5-[5-(propylsulfanylcarbonyl)pyridin-2-yl]-5,7-dihydrofuro[3,4-*b*]pyridine-2-carbothioate (**4j**) (0.40 g, 35%). (Yields by ^1H NMR spectroscopy.) The very similar R_f values of these compounds made purification difficult.

(**4f**), TLC [diethyl ether–light petroleum (bp 60–90 °C) (1:1)] R_f 0.50; mp 44–45 °C (Found: C, 55.19; H, 5.79; N, 6.04; S, 13.64. $C_{11}H_{13}NO_3S$ requires C, 55.21; H, 5.48; N, 5.85; S, 13.40%); ν_{max}(KBr)/cm^{-1} 1724 [O–C(O)] and 1668 [S–C(O)]; δ_H(300 MHz; $CDCl_3$) 1.02 (3 H, t, *J* 7.3, CH_2CH_3), 1.70 (2 H, m, *J* 7.2, CH_2CH_3), 3.01 (2 H, t, *J* 7.1, S–CH_2), 4.01 (3 H, s, O–CH_3), 7.98 (1 H, t, *J* 7.5, Ar 4-H), 8.10 (1 H, d, *J* 6.9, Ar H) and 8.29 (1 H, d, *J* 7.9, Ar H); δ_C(300 MHz; $CDCl_3$) 13.55 (CH_2CH_3), 22.61 (CH_2CH_3), 30.69 (S–CH_2), 53.14 (O–CH_3), 123.10 (Ar C-5), 128.617 (Ar C-3), 138.40 (Ar C-4), 147.57 (Ar C-2), 152.11 (Ar C-6), 164.87 [O–C(O)] and 193.12 [S–C(O)]; *m/z* 239 (M^+, 1%), 211 (13), 165 (11), 137 (100), 105 (21), 77 (17), 59 (19) and 41 (13).

(**4j**), TLC [diethyl ether–light petroleum (bp 60–90 °C) (1:1)] R_f 0.45; mp 97–98 °C (Found: C, 58.80; H, 5.27; N, 6.48; S, 14.85. $C_{21}H_{22}N_2O_4S_2$ requires C, 58.58; H, 5.15; N, 6.51; S, 14.89%); ν_{max}(KBr)/cm^{-1} 1793 [O–C(O)] and 1667 [S–C(O)]; δ_H[300 MHz; $(CD_3)_2SO$] 0.94–0.99 (6 H, m, 2 CH_2CH_3), 1.58–1.67 (4 H, m, 2 CH_2CH_3), 2.12 (3 H, s, CH_3), 2.92–3.03 (4 H, m, 2 S–CH_2), 7.86 (1 H, d, *J* 7.8, Ar H), 7.94 (1 H, d, *J* 8.0, Ar H), 8.11 (1 H, t, *J* 7.8, Ar H), 8.29 (1 H, d, *J* 8.1, Ar H) and 8.61 (1 H, d, *J* 8.1, Ar H); δ_C[300 MHz; $(CD_3)_2SO$] 13.25 and 13.38 (2 CH_2CH_3), 22.33 and 22.48 (2 CH_2CH_3), 26.19 (CH_3), 29.94 and 30.14 (2 S–CH_2), 86.06 (quaternary C), 119.78, 124.45, 124.53, 134.72, 140.13, 143.18, 149.95, 150.40, 154.15 and 157.92 (Ar C), 165.78 [O–C(O)], 192.11 and 192.66 [2 S–C(O)]; DEPT[25] δ_C[300 MHz; $(CD_3)_2SO$] 13.25, 13.38 and 26.19 (CH_3), 22.33, 22.48, 19.94 and 30.14 (CH_2), 119.78, 124.45, 124.53, 134.72 and 140.13 (CH); *m/z* 430 (M^+, 4%), 386 (1), 360 (9), 328 (18), 300 (17), 253 (27), 226 (44), 195 (7), 181 (13), 140 (16), 126 (9), 76 (10) and 43 (100).

Acknowledgements

We thank Mrs M. Bates and Dr L. Deady for providing compounds **5–8** and for assistance in the synthesis of com-

pound **4a**. Grateful acknowledgement also is given to Dr K. Ang for assistance with the chromatography experiments and discussion of NMR data, Dr D. Fiedler for assistance in acquiring the EPR spectra and the Australian Research Council for financial support for part of this project.

References

1 H. Lund and M. M. Baizer, *Organic Electrochemistry*, Marcel Dekker, New York, 1991.
2 J. H. Wagenknecht, R. D. Goodin, P. J. Kinlin and F. O. Woodard, *J. Electrochem. Soc.*, 1984, **131**, 1559.
3 M. Falsig and H. Lund, *Acta Chem. Scand., Ser. B*, 1980, **34**, 585.
4 C. Praefcke, C. Weichsel, M. Falsig and H. Lund, *Acta Chem. Scand., Ser. B*, 1980, **34**, 403.
5 J. Voss, C. Von Bülow, T. Drews and P. Mischke, *Acta Chem. Scand., Ser. B*, 1983, **37**, 519.
6 A. Streitwieser, *Molecular Orbital Theory For Organic Chemists*, Wiley, New York, 1961, ch. 7.
7 A. J. Bard and L. R. Faulkner, *Electrochemical Methods*, Wiley, New York, 1980, p. 160.
8 R. S. Nicholson and I. Shain, *Anal. Chem.*, 1964, **36**, 706; R. S. Nicholson, *Anal. Chem.*, 1966, **38**, 1406.
9 D. Barnes and P. Zuman, *J. Chem. Soc., Faraday Trans.*, 1969, **65**, 1668.
10 T. Awata, M. M. Baizer, T. Nonaka and T. Fuchigami, *Chem. Lett.*, 1985, 371.
11 V. P. Gul'tyai, T. Ya. Rubinskaya and L. M. Korotaeva, *Bull. Pol. Acad. Sci. Chem.*, 1982, 1499, cited from ref. 2.
12 R. B. Moll, E. J. Poziomek and W. A. Mosher, *J. Org. Chem.*, 1971, **36**, 1056; J. Holubek and J. Volke, *Collect. Czech. Chem. Commun.*, 1960, **25**, 3292.
13 K. Boujlel and J. Simonet, *Tetrahedron Lett.*, 1979, 1063.
14 F. Magno and G. Bontempelli, *J. Electroanal. Chem.*, 1976, **68**, 337; J. San Filippo, Jr., L. J. Romano, C.-I. Chern and J. S. Valantino, *J. Org. Chem.*, 1976, **68**, 337; M. J. Gibian, D. T. Sawyer, T. Ungermann, R. Tangpoonpholvivat and M. M. Morrison, *J. Am. Chem. Soc.*, 1979, **101**, 640; D. T. Sawyer and J. S. Valentine, *Acc. Chem. Res.*, 1981, **14**, 393.
15 J. C. Sheehan and G. F. Holland, *J. Am. Chem. Soc.*, 1956, **78**, 5631.
16 F. Gerson, *High Resolution E.S.R. Spectroscopy*, Wiley, New York, 1967, ch. 2.
17 M. Hirayama, *Bull. Chem. Soc. Jpn.*, 1967, **40**, 1822.
18 J. Pilbrow, Monash University, personal communication.
19 J. A. Weil, J. R. Bolton and J. E. Wertz, *Electron Paramagnetic Resonance*, Wiley-Interscience, New York, 1994, p. 511.
20 M. Bates, La Trobe University, unpublished work.
21 M. M. Bates, T. J. Cardwell, R. W. Cattrall, L. W. Deady and K. Murphy, *Aust. J. Chem.*, 1991, **44**, 1603.
22 T. Osa and T. Kuwana, *J. Electroanal. Chem.*, 1969, **22**, 389; A. J. Fry and W. E. Britton in *Laboratory Techniques in Electroanalytical Chemistry*, ed. P. T. Kissinger and W. R. Heineman, Marcel Dekker, New York, 1984, ch. 13.
23 D. Fiedler, M. Koppenol and A. M. Bond, *J. Electrochem. Soc.*, 1995, **142**, 862.
24 P. Delahay, *New Instrumental Methods in Electrochemistry*, Interscience, New York, 1954, p. 392.
25 D. M. Doddrell, D. T. Pegg and M. R. Bendall, *J. Magn. Reson.*, 1982, **48**, 323.

Paper 5/00402K
Received 24*th January* 1995
Accepted 21*st February* 1995